Virologica Sinica 38 (2023) 900–910

Contents lists available at ScienceDirect

Virologica Sinica

journal homepage: www.keaipublishing.com/en/journals/virologica-sinica
www.virosin.org

Research Article

Classical swine fever virus NS5A protein antagonizes innate immune response by inhibiting the NF-κB signaling

Jinfu Sun [a,*], Jiaying Li [a], Liming Li [a], Haixiao Yu [a], Ping Ma [a], Yingnan Wang [a], Jinqi Zhu [a], Zezhong Feng [a], Changchun Tu [b,c,*]

[a] Key Laboratory of Bioresource Research and Development of Liaoning Province, College of Life and Health Sciences, Northeastern University, Shenyang, 110169, China
[b] Changchun Veterinary Research Institute, Chinese Academy of Agricultural Sciences, Changchun, 130122, China
[c] Jiangsu Co-innovation Center for Prevention and Control of Important Animal Infectious Disease and Zoonoses, Yangzhou University, Yangzhou, 225009, China

ARTICLE INFO

Keywords:
Classical swine fever virus (CSFV)
NS5A
NF-κB signaling
NEMO
Polyubiquitination
Proteasomal degradation

ABSTRACT

The NS5A non-structural protein of classical swine fever virus (CSFV) is a multifunctional protein involved in viral genomic replication, protein translation, assembly of infectious virus particles, and regulation of cellular signaling pathways. Previous report showed that NS5A inhibited nuclear factor kappa B (NF-κB) signaling induced by poly(I:C); however, the mechanism involved has not been elucidated. Here, we reported that NS5A directly interacted with NF-κB essential modulator (NEMO), a regulatory subunit of the IκB kinase (IKK) complex, to inhibit the NF-κB signaling pathway. Further investigations showed that the zinc finger domain of NEMO and the aa 126–250 segment of NS5A are essential for the interaction between NEMO and NS5A. Mechanistic analysis revealed that NS5A mediated the proteasomal degradation of NEMO. Ubiquitination assay showed that NS5A induced the K27-linked but not the K48-linked polyubiquitination of NEMO for proteasomal degradation. In addition, NS5A blocked the K63-linked polyubiquitination of NEMO, thus inhibiting IKK phosphorylation, IκBα degradation, and NF-κB activation. These findings revealed a novel mechanism by which CSFV inhibits host innate immunity, which might guide the drug design against CSFV in the future.

1. Introduction

Classical swine fever (CSF) is an economically important swine viral disease characterized by acute hemorrhagic fever, high morbidity and mortality, or atypical, inapparent clinical manifestations, depending on the virulence of the virus strain (Muñoz-González et al., 2015). The causative agent, CSF virus (CSFV) is a member of the genus *Pestivirus* within the family *Flaviviridae*. The CSFV genome contains a large open reading frame (ORF) that encodes a polyprotein, which is cleaved by cellular and viral proteases into four structural proteins (C, E^{rns}, E1, and E2) and eight nonstructural proteins (N^{pro}, p7, NS2, NS3, NS4A, NS4B, NS5A and NS5B) (Tautz et al., 2015).

Pestivirus NS5A, a multifunctional protein with RNA binding activity, is the only replication complex component that can be complemented *in trans* (Grassmann et al., 2001). Bovine viral diarrhea virus (BVDV) NS5A contains a zinc-binding motif which is essential for viral RNA replication (Tellinghuisen et al., 2006). The N-terminal amphipathic alpha-helix of BVDV NS5A anchors the protein to the intracellular membrane, which is necessary for the formation of viral replication complex (Sapay et al., 2006). CSFV NS5A is a 55 kDa protein containing a conserved sequence (C2717-C2740-C2742-C2767), which plays critical roles in viral RNA replication, protein translation, and virus assembly (Sheng et al., 2010). CSFV NS5A regulates viral RNA replication by binding to the 3′-UTR and NS5B (Sheng et al., 2012; Chen et al., 2012b). It also participates in virus assembly by interacting with viral core protein (Sheng et al., 2014), or with host proteins such as annexin A2 (Sheng et al., 2015) and Rab18 (Zhang et al., 2020). In addition, CSFV NS5A suppresses the secretion of inflammatory cytokines by inhibiting the NF-κB signaling pathway (Dong and Tang, 2016).

NF-κB plays a critical role in inflammatory immune responses, cell growth, and apoptosis (Napetschnig and Wu, 2013). In unstimulated cells, NF-κB is sequestered in the cytoplasm by associating with inhibitory IκB proteins (IκBs), which mask the nuclear localization signal of NF-κB. Upon stimulation with tumor necrosis factor (TNF)-α, TNF receptor 1 (TNFR1) recruits TNF receptor associated death domain protein (TRADD) and the receptor-interacting protein 1 (RIP1) kinase. TRADD further recruits the E3 ubiquitin ligases of TNF receptor-associated factor 2 (TRAF2) and cellular inhibitor of apoptosis proteins (cIAP1 and cIAP2)

* Corresponding authors.
E-mail addresses: sunjinfu@mail.neu.edu.cn (J. Sun), changchun_tu@hotmail.com (C. Tu).

https://doi.org/10.1016/j.virs.2023.09.002
Received 11 February 2023; Accepted 8 September 2023
Available online 14 September 2023

to TNFR1, which then mediates K63-linked polyubiquitination of RIP1 (Alvarez et al., 2010; Bertrand et al., 2008). The polyubiquitinated RIP1 recruits transforming growth factor-β-activated kinase 1 (TAK1) to TNF receptor complex, and then TAK1 is activated by the K63-linked polyubiquitination (Fan et al., 2010; Wang et al., 2001; Takaesu et al., 2003). The IκB kinase (IKK) complex, which consists of catalytic subunits (IKKα and IKKβ) and regulatory subunit IKKγ (NF-κB essential modulator, NEMO), is also recruited to TNF receptor complex by RIP1 through the association between the polyubiquitin chains and NEMO. Subsequently, TAK1 phosphorylates and activates IKK complex (Ea et al., 2006; Wajant and Scheurich, 2011). Upon activation, IKK phosphorylates IκBs, which triggers IκBs polyubiquitination and proteasomal degradation. The degradation of IκBs allows NF-κB to translocate to the nucleus and activate specific target gene transcription.

Upon viral infection, cellular pattern recognition receptors recognize viral pathogen-associated molecular patterns. This process rapidly induces host innate and subsequent adaptive immune responses, leading to viral suppression (Iwasaki and Medzhitov, 2010). The activation of NF-κB plays a critical role in the immediate early events of innate immune responses and in the inflammatory responses following microbial infection (Dev et al., 2011; Le Negrate, 2012). Viruses have therefore evolved various mechanisms targeting the NF-κB signaling pathway to evade host innate immune response (Zhuo et al., 2021). As for CSFV, Chen et al. (2012a) found that CSFV virulent strain and attenuated Thiverval strain failed to activate NF-κB signaling both in PBMC of infected pigs and in PK-15 cells. This team also reported that CSFV activated NF-κB and IRF3 signaling by upregulation of RIG-1 and MDA5 in porcine alveolar macrophages (Dong et al., 2013), which showed different regulations of the NF-κB signaling by CSFV in various cells. Li et al. (2015) suggested that CSFV E2 inhibited thioredoxin-2-mediated NF-κB signaling by reducing the expression of thioredoxin-2. Dong and Tang (2016) showed that CSFV NS5A inhibited NF-κB signaling and inflammatory cytokine IL-1β, IL-6 and TNF-α expression induced by poly(I:C) and did not affect the expression levels of RIG-I, MDA5, IPS-1, NF-κB and IκBα in PAM cells without poly(I:C) stimulation. However, the mechanism of the inhibition of NF-κB signaling by NS5A has not been elucidated. Our previous study screened the host target proteins of CSFV NS5A, and found that NEMO was one of the NS5A binding partners. In this study, we aim to investigate the interaction between NS5A and NEMO, and reveal the mechanism by which NS5A inhibits NF-κB signaling.

2. Materials and methods

2.1. Cells and virus strain

Pig kidney cell line PK-15 and human embryonic kidney HEK293T cells were maintained in Dulbecco's modified Eagle's medium (DMEM) (Sigma, St. Louis, MO, USA) and porcine alveolar macrophages (PAMs) were maintained in 1640 medium (Sigma, St. Louis, MO, USA) containing 10% fetal bovine serum (FBS; Gibco-BRL, Gaithersburg, MD, USA), 100 U/mL penicillin G (Thermo Fisher Scientific, USA) and 100 μg/mL streptomycin sulfate (Thermo Fisher Scientific, USA). The serum was negative for bovine viral diarrhea virus (BVDV) and BVDV antibody. PK-15 cells of 80%–90% confluent in 6-well cell culture plates (Corning, NY, USA) were infected with the CSFV Shimen strain (GenBank accession number AF092448.2) at a multiplicity of infection (MOI) of 1 for examining the interaction of native NS5A and NEMO, and at an MOI of 3 and 5 for examining NEMO degradation, and then further cultured in DMEM containing 2% FBS.

2.2. Antibodies and reagents

Mouse anti-Flag monoclonal antibody (mAb) (66008-3-Ig), rabbit anti-Flag polyclonal antibody (20543-1-AP), mouse anti-GAPDH mAb (60004-1-Ig), mouse anti-NEMO mAb (66460-1-Ig), mouse anti-HA tag mAb (66006-2-Ig), mouse anti-His tag mAb (66005-1-Ig) and rabbit anti-Myc polyclonal antibody (10828-1-AP) were purchased from Proteintech. Rabbit anti-NEMO mAb (ab230832) were purchased from Abcam (Cambridge, UK). K48-linkage specific polyubiquitin (D9D5) rabbit mAb (8081), K63-linkage specific polyubiquitin (D7A11) rabbit mAb (5621), ubiquitin (P4D1) mouse mAb (3936), phosphor-IKK (Ser176/180) (16A6) rabbit mAb (2697) were purchased from Cell Signaling Technology (Danvers, MA, USA). Rabbit anti-NS5A serum and mouse anti-E2 mAb was prepared in our laboratory. TNF-α (SC-4564) was purchased from Santa Cruz Biotechnology (CA, USA). MG132 (HY-13259) and N-ethylmaleimide (HYD0843) were purchased from MedChemExpress (NJ, USA). Lipofectamine™ 3000 Transfection Reagent (L3000075), Dynabeads™ Protein G Immunoprecipitation Kit (10007D), Dynabeads™ His-Tag isolation and pulldown (10104D) were purchased from Thermo Fisher Scientific (MA, USA).

2.3. Construction of plasmids

Construction of pET-NS5A and p3×FLAG-NS5A plasmids was described previously (Liu et al., 2018). Four truncated mutants of NS5A (NS5Am1, NS5Am2, NS5Am3, and NS5Am4) were amplified by PCR and inserted into the *Eco*RI and *Bam*HI sites of p3×FLAG-CMV-10 vector to produce recombinant expression vectors of p3×FLAG-NS5Am1, p3×FLAG-NS5Am2, p3×FLAG-NS5Am3, and p3×FLAG-NS5Am4. The *NEMO* gene was synthesized and cloned into the *Eco*RI and *Xho*I sites of pcDNA3.1/*myc*-His A vector (Invitrogen, Carlsbad, CA, USA) to construct the pcDNA-NEMO vector. Four truncated mutants of NEMO (ΔN1, ΔN2, ΔN3, and ΔN4) were amplified by PCR and inserted into the *Eco*RI and *Kpn*I sites of pCMV-Myc vector to produce pCMV-NEMOΔN1, pCMV-NEMOΔN2, pCMV-NEMOΔN3, and pCMV-NEMOΔN4. Wild type ubiquitin and ubiquitin mutants' sequences (K6, K11, K27, K29, K33, and K63) were synthesized and inserted into the *Eco*RI and *Xho*I sites of pCMV-HA vector to produce pCMV-HA-Ub, pCMV-HA-K6Ub, pCMV-HA-K11Ub, pCMV-HA-K27Ub, pCMV-HA-K29Ub, and pCMV-HA-K33Ub. Each mutant contained only one lysine (K) residue, while the six others were replaced by arginine (R). The ubiquitin mutant *K27RUb* gene was amplified by overlapping PCR and was inserted into the *Eco*RI and *Xho*I sites of the pCMV-HA vector to produce pCMV-HA-K27RUb. The primers used in present study were listed in Supplementary Table S1.

2.4. Co-immunoprecipitation (Co-IP) assay

Cells in 6-well plates were transfected with recombinant plasmid p3×FLAG-NS5A, NS5A mutants or other indicated expression vectors (2.5 μg/well) using Lipo8000 (Beyotime, Shanghai, China) according to the manufacturer's directions. At 48 h post-transfection, cells were lysed and subjected to Co-IP with Dynabeads™ Protein G (Thermo Fisher Scientific, Waltham, MA, USA) and indicated antibodies followed by the protocols as described previously (Liu et al., 2018).

2.5. His tag pull down assay

Pull down assay was conducted as described previously (Liu et al., 2018). Briefly, Dynabeads™ (Thermo Fisher) with bound His-NS5A or His tag were incubated with the cell lysates from HEK293T cells expressing Myc-NEMOΔN1, Myc-NEMOΔN2, Myc-NEMOΔN3 or Myc-NEMOΔN1 for 10 min on a roller at 37 °C. Proteins co-purified with His-NS5A or His-tagged protein were detected by western blotting with rabbit anti-Myc polyclonal antibody (Proteintech, China) for probing NEMO mutants and mouse anti-His tag mAb (Proteintech, China) for probing NS5A.

2.6. Western blotting

Cells were lysed and proteins were extracted, 25 μg of protein was mixed with an equal volume of SDS-PAGE loading buffer, then boiled for

5 min. After separation by SDS-PAGE, the proteins were transferred to PVDF membranes (Millipore Corp., Mass., USA). Following blocking with buffer (1% BSA in 0.01 mol/L PBS, pH 7.4) for 2 h at 37 °C, the membranes were then incubated for 2 h at 37 °C with primary antibodies. After washing three times with PBST, the membranes were further incubated with secondary antibody conjugated with horseradish peroxidase at 37 °C for 2 h. After washing with PBST, reactive protein stripes were visualized using the BeyoECL Plus kit (Beyotime, China).

2.7. NF-κB transcriptional activity

HEK293T cells in 24-well plates were transfected with p3×FLAG-NS5A, p3×FLAG-NS5Am1, p3×FLAG-NS5Am2, p3×FLAG-NS5Am3, p3×FLAG-NS5Am4, or p3×FLAG-CMV-10 vector at 0.5 μg per well along with pNF-κB-Luc (Beyotime, China) of 0.5 μg and pRL-TK (Beyotime) of 0.25 μg per well. At 48 h post-transfection, the cells were stimulated with or without TNF-α (final concentration 20 ng/mL) for 15 min and then harvested for firefly luciferase (FLuc) and Renilla luciferase (RLuc) activities assay using the Dual-Lumi Luciferase Reporter Gene Assay Kit (Beyotime).

2.8. Real-time RT-PCR

HEK293T cells in 24-well plates were transfected with p3×FLAG-NS5A, p3×FLAG-NS5Am1, p3×FLAG-NS5Am2, p3×FLAG-NS5Am3, p3×FLAG-NS5Am4 or p3×FLAG-CMV-10 vector of 0.5 μg per well. At 48 h post-transfection, the cells were stimulated with or without TNF-α (final concentration of 20 ng/mL) for 15 min and then harvested for quantification of IFN-α mRNA using the One-Step SYBR Prime Script RT-PCR kit (TaKaRa, Dalian, China) according to the manufacturer's protocol. Briefly, the total RNA was isolated from TNF-α treated or untreated HEK293T cells with TRIzol reagent (TaKaRa, Dalian, China). cDNA was synthesized from 1 μg of total RNA with Prime Script II (TaKaRa, Dalian, China). Quantitative real-time PCR analysis was performed using an ABI PRISM 7000 cycler (Applied Biosystems, Carlsbad, CA, USA) and Fast-Start Universal SYBR Green Master (TaKaRa). The level of α-tubulin expression was used to normalize the data. The primers were listed in Supplementary Table S1.

2.9. Ubiquitination assay

PK-15 cells or HEK293T cells in 6-well plates were transfected with p3×FLAG-NS5A or p3×FLAG-CMV-10 (2.5 μg/well) and vectors (2.5 μg/well) expressing HA tag, wild-type ubiquitin (WT-Ub), or Ub mutant (K6, K11, K27, K29, K33, and K63). Then the cells were incubated with MG132 (MedChemExpress, 10 μmol/L) for 24 h and infection with Sendai virus (SeV) (500 HAU/well) for 12 h. At 48 h post-transfection, the cells were lysed with lysis buffer containing 10 μmol/L deubiquitinating enzyme inhibitor of N-ethylmaleimide (MCE) for immunoprecipitation with rabbit anti-NEMO mAb (Abcam). Precipitated proteins were subjected to Western blotting with mouse anti-Ub mAb (CST), K48-linkage specific polyubiquitin (D9D5) rabbit mAb (CST, USA), mouse anti-HA mAb (Proteintech), or K63-linkage specific polyubiquitin (D7A11) rabbit mAb (CST, USA), respectively.

2.10. MTT assay

To evaluate the effects of MG132 treatment on the cell viability, MTT assay was conducted using MTT Cell Proliferation and Cytotoxicity Assay Kit (Beyotime, China) according to the introduction manual.

2.11. Statistical analysis

All experiments were conducted with at least three independent replicates. Experimental data were analyzed by GraphPad Prism software using Student's *t*-test. Differences in data were regarded as significant if $P < 0.05$.

3. Results

3.1. NS5A interacts with cellular NEMO

In our previous study, host partners binding to CSFV NS5A were screened via the His-tag pull-down assay and LC–MS/MS identification (Liu et al., 2018). In the present study, NEMO, one binding partner of NS5A, was selected for further analysis because of its critical roles in the NF-κB signaling pathway. The interaction between NS5A and endogenous NEMO was confirmed in HEK293T cells expressing FLAG-NS5A fusion protein by Co-IP. Results indicated that NEMO specifically co-precipitated with the fusion protein FLAG-NS5A but not FLAG tag (Fig. 1A and B). The interaction between NS5A produced by virus infection and endogenous NEMO was also validated in CSFV-infected PK-15 cells by Co-IP assay (Fig. 1C).

3.2. The domain on NEMO required for the NEMO–NS5A interaction

NEMO is composed of several overlapping function domains, the IKK-binding domain, two coiled-coil domains (CC1 and CC2), a leucine zipper (LZ), a ubiquitin-binding domain, and a C-terminal zinc finger (ZF) (Chiaravalli et al., 2011). To explore the potential effects of the interaction between NS5A and NEMO on the function of NEMO, the region of NEMO required for interaction with NS5A was determine by His pull-down assay. HEK293T cells were transfected with truncated mutants of NEMO (pCMV-NEMOΔN1, pCMV-NEMOΔN2, pCMV-NEMOΔN3 or pCMVNEMOΔN4) (Fig. 2A) and collected at 48 h post-transfection for pull down assay. The results showed that only NEMOΔN3 (aa 126–419) mutant, but not NEMOΔN1 (aa 1–290), NEMOΔN2 (aa 1–350) or NEMOΔN4 (aa 221–419), was pulled down by NS5A (Fig. 2B), indicating that the N terminal region aa 1–125 of NEMO containing the IKKα/β binding domain (aa 50–93) (May et al., 2000) was unnecessary for the interaction between NS5A and NEMO. However, aa 126–220 in CC1 domain and aa 351–419 containing the ZF domain which are essential for K63 polyubiquitination of NEMO were at least required.

3.3. The region of NS5A required for the NS5A–NEMO interaction

HEK293T cells expressing the full-length NS5A or one of the four truncated mutants NS5Am1 (aa 1–250), NS5Am2 (aa 251–497), NS5Am3 (aa 1–428), and NS5Am4 (aa 126–497) (Fig. 3A) were lysed for co-IP assay. The results showed that only NS5Am2 (deletion of aa 1–250 region) did not interact with NEMO (Fig. 3B), which indicated that the aa 126–250 region in NS5A is responsible for its interaction with NEMO.

3.4. The NS5A region required for inhibition of NF-κB signaling

Previous study showed that CSFV NS5A could inhibit poly(I:C)-induced IκBα degradation thus further suppress the NF-κB nuclear translocation and activity in PAMs (Dong and Tang, 2016). Here we confirmed the NS5A region required for the inhibition of NF-κB signaling in full-length or truncated NS5A transfected HEK293T cells. About 48 h post-transfection, the cells were treated with or without TNF-α for 15 min, and then the cells were lysed for the detection of phosphorylated IKKα/β, IκBα, and IFN-α. The results indicated that only the NS5Am2 mutant failed to inhibit IKKα/β phosphorylation (Fig. 4A), IκBα degradation (Fig. 4B), and IFN-α mRNA expression (Fig. 4C).

To determine NS5A region required for the inhibition of NF-κB transcriptional activity, NS5A or its truncated mutants were co-transfected with NF-κB Luc reporter plasmid and PRL-TK plasmid in HEK293T cells. After 48 h, the cells were stimulated with or without TNF-α for 15 min, and then NF-κB transcriptional activity was assayed. The results suggested that only the NS5Am2 mutant did not inhibit NF-κB

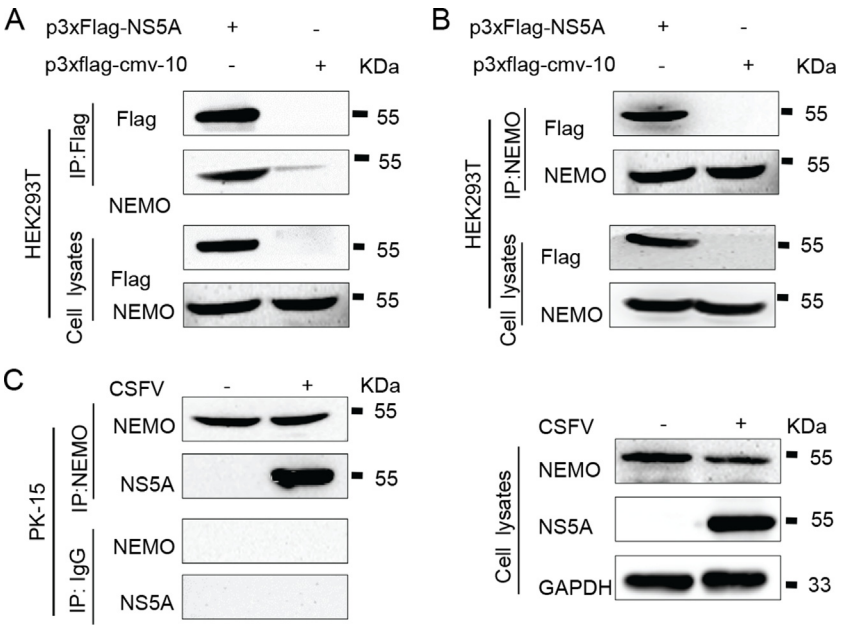

Fig. 1. The CSFV NS5A interacts with NEMO. **A, B** HEK293T cells in 6-well plates were transfected with p3×FLAG-NS5A or p3×FLAG-CMV-10 (2.5 μg/well). At 48 h post-transfection, the cells were lysed for co-immunoprecipitation (co-IP) and Western blotting with indicated antibodies. **C** PK15 cells were infected with CSFV Shimen strain at an MOI of 1. At 48 hpi, the cells were lysed for co-IP and Western blotting with indicated antibodies.

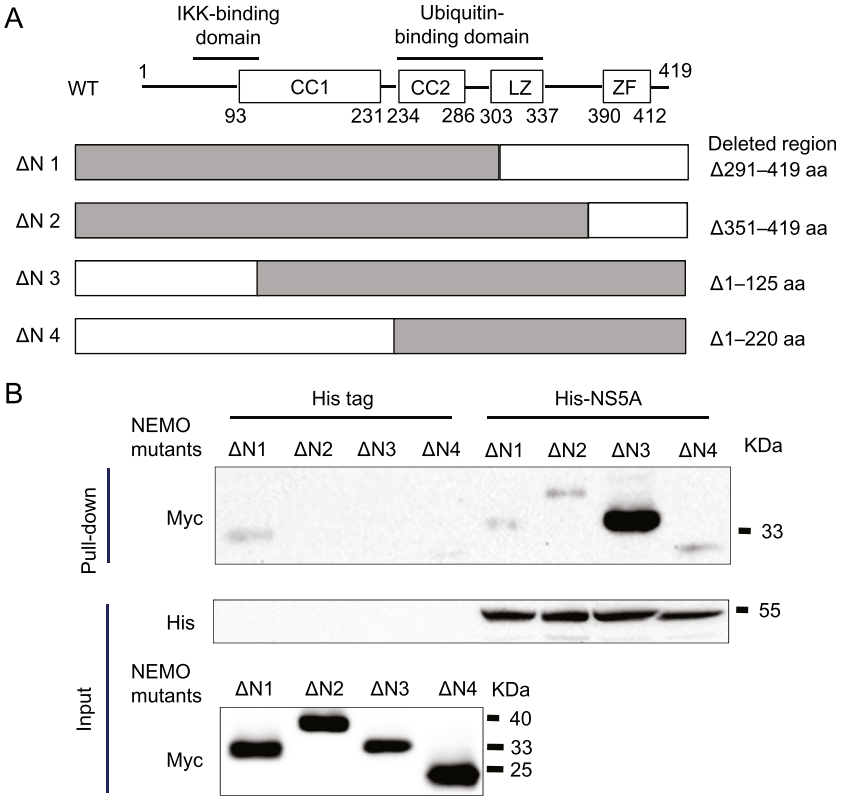

Fig. 2. Determination of the domain of NEMO required for the association with NS5A. **A** Schematic representation of NEMO mutant constructs. **B** HEK293T cells in 6-well plates were transfected with NEMO mutants (2.5 μg/well). After 48 h of transfection, the cells were lysed and incubated with Dynabeads™ coupled with His-NS5A or His tag. The proteins co-purified with fusion protein His-NS5A or His tag and cell lysates were subjected to Western blotting analysis using the indicated antibodies.

transcriptional activity induced by TNF-α (Fig. 4D). These data indicated that the aa 126–250 region of NS5A was essential for the inhibition of IKK and NF-κB activation by NS5A. The expression level of NS5A and its truncated mutants in above experiments is shown in Fig. 4E.

3.5. The decrease of NEMO induced by CSFV or NS5A

NS5A inhibits the NF-κB signaling pathway during CSFV infection, thus we further explored the detailed mechanism, especially the role of

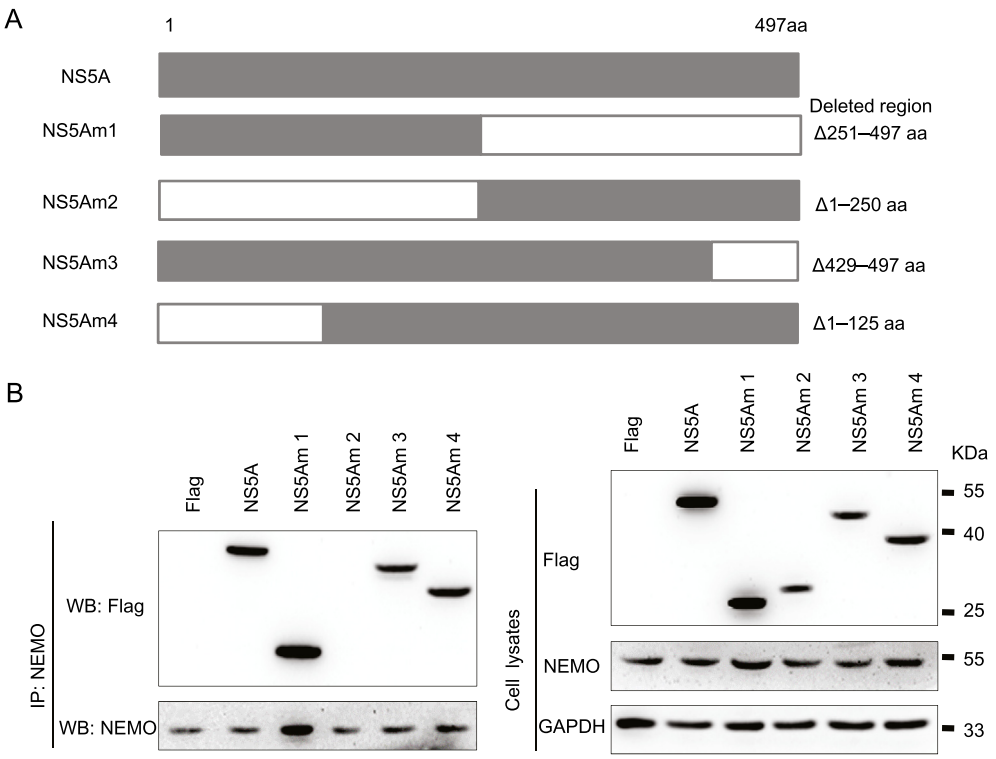

Fig. 3. Determination of the region of NS5A required for NS5A-NEMO interaction. **A** Schematic representation of NS5A mutant constructs. **B** HEK293T cells in 24-well plates were transfected with full-length NS5A or NS5A truncated mutant (1 μg/well). FLAG tag was used as control. After 48 h of transfection, the cells were lysed for co-immunoprecipitation and Western blotting assay with the indicated antibodies.

NEMO in this process. The expression level of NEMO was first determined after CSFV infection. PK-15 cells (Fig. 5A) or PAM cells (Fig. 5B) were infected with the CSFV Shimen (virulent) strain at an MOI of 3 and 5, and the expression level of NEMO was analyzed by Western blotting at 48 hpi. The results showed that NEMO protein level progressively decreased with the increase of MOI (Fig. 5A and B).

The decrease of NEMO induced by NS5A was further confirmed in NEMO-NS5A co-transfected and NS5A-transfected HEK293T cells. Results showed that the levels of NEMO progressively decreased with the increase of NS5A expression in the cells with exogenous NEMO expression (Fig. 5C), and the endogenous NEMO was also decreased as the expression of NS5A increased (Fig. 5D).

3.6. NS5A mediates the proteasomal degradation of NEMO

Both proteasomical and lysosomical degradation systems are the most important proteolytic pathways in cells (Wang and Robbins, 2014; Ciechanover, 2005). To reveal the mechanism of the decrease of NEMO mediated by NS5A, the possibility that NS5A mediates the proteasomal degradation of NEMO was first examined using the proteasome inhibitor MG132. As shown in Fig. 6A, NEMO protein levels progressively increased with increasing MG132 concentrations in cells with exogenous NEMO and NS5A expression. MG132 also inhibited the endogenous NEMO degradation mediated by NS5A (Fig. 6B). These data indicated that NS5A induced proteasomal degradation of NEMO. Fig. 6C showed the effects of MG132 on cell viability.

3.7. NS5A induces the NEMO ubiquitination but does not mediate the K48-linked polyubiquitination of NEMO

Protein ubiquitination is required for proteasomal degradation. To test whether NS5A induces NEMO ubiquitination, PK-15 cells and HEK293T cells were transfected with p3×FLAG-NS5A or p3×FLAG-CMV-10 and then incubated with MG132 for 24 h. At 48 h post-transfection, the cells were lysed for immunoprecipitation and Western blotting with indicated antibodies. The result showed that ubiquitinated NEMO was increased in NS5A-expressed cells, indicating that NS5A induces NEMO ubiquitination (Fig. 7).

The K48-linked polyubiquitination usually triggers proteasomal degradation. The role of K48-linked polyubiquitination in NS5A-mediated NEMO degradation was investigated by the ubiquitination assay of NEMO. Results suggested that the level of K48-linked polyubiquitination of NEMO in the NS5A-expressing PK-15 cells or HEK293 cells was similar to that in control cells, thus NS5A did not mediate the K48-linked polyubiquitination of NEMO (Fig. 8).

3.8. NS5A induces the K27-linked polyubiquitination of NEMO

To identify the type of polyubiquitination of NEMO for proteasomal degradation, ubiquitin (Ub) mutant genes (K6, K11, K27, K29, K33, and K63) were synthesized. PK-15 cells (Fig. 9A and B) and HEK293T cells (Fig. 9C and D) were co-transfected with NS5A and WT-Ub or Ub mutant, and the ubiquitination assay of NEMO was performed at 48 h post-transfection. The results showed a marked enhancement of polyubiquitination of NEMO in cells expressing wild-type HA-Ub or mutant HA-K27-Ub, while the polyubiquitination of NEMO in cells expressing other Ub mutant is similar to that in control cells expressing HA tag (Fig. 9A and C). Next, the plasmid pCMV-HA-K27RUb expressing ubiquitin bearing k27R mutation was used to further validate that NS5A induces K27-linked polyubiquitination of NEMO. The results indicated that polyubiquitination of NEMO was eliminated in the cells expressing the HA-K27R-Ub mutant compared to that in cells expressing WT-Ub (Fig. 9B and D). These data indicate that NS5A induces the K27-linked polyubiquitination of NEMO for proteasomal degradation.

3.9. NS5A inhibits the K63-linked polyubiquitination of NEMO

As shown in Fig. 2B, the NEMO C-terminal region of aa 351–419 containing a zinc finger (ZF) domain is necessary for the interaction of

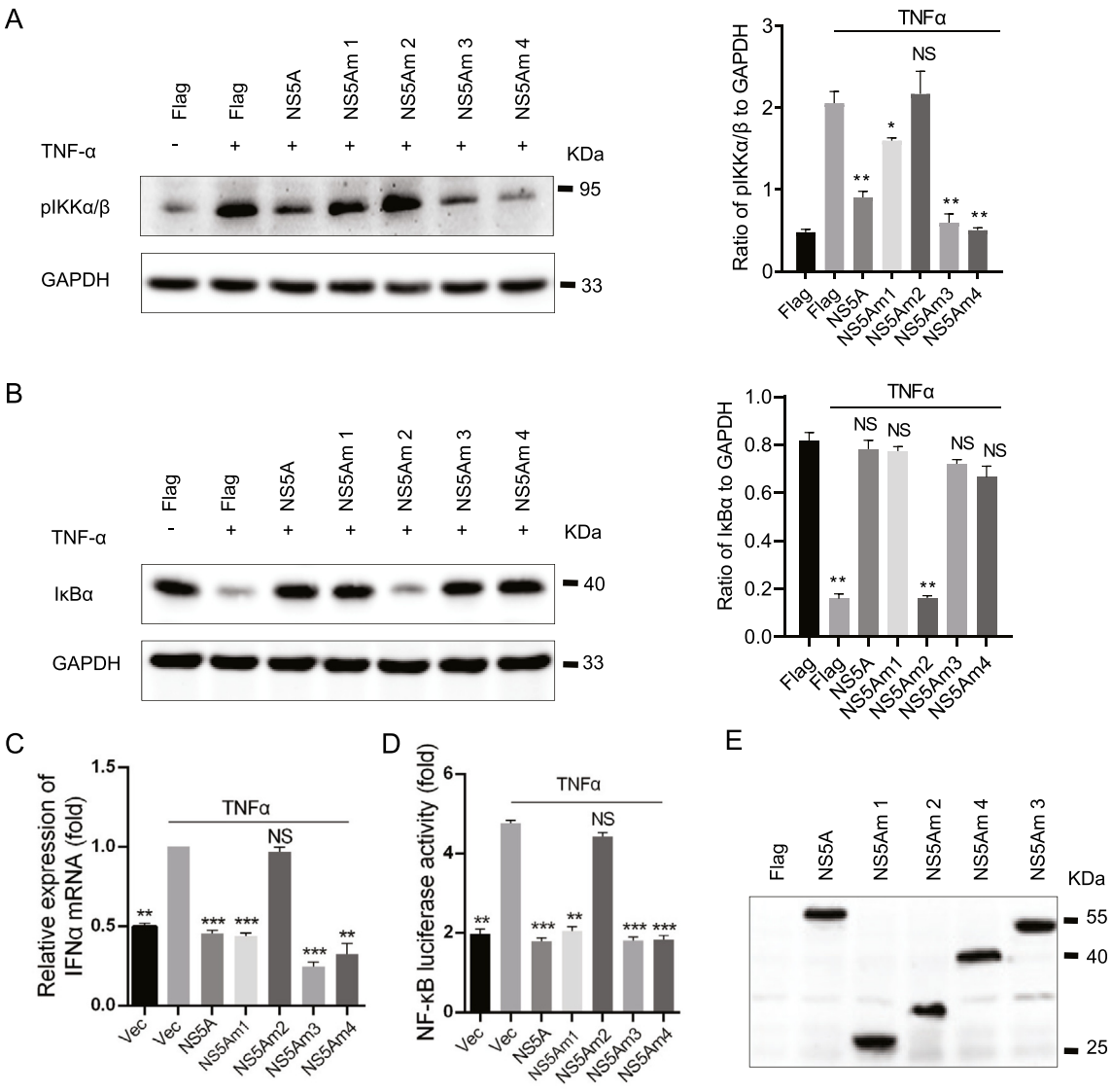

Fig. 4. Determination of the region of NS5A required for inhibition of the NF-κB signaling. **A–C** HEK293T cells in 6-well plate were transfected with full-length NS5A or NS5A truncated mutant (2.5 μg/well). After 48 h, the cells were treated with or without TNF-α for 15 min and then harvested for detection of IKKα/β phosphorylation (**A**), IκBα degradation (**B**), quantification of IFN-α mRNA (**C**). The expressing level of phosphorylated IKKα/β and IκBα was analyzed by Western blotting. IFN-α mRNA was detected by RT-PCR using the One-Step SYBR Prime Script RT-PCR kit. **D** HEK293T cells in 24-well plate were transfected with pNF-κB-Luc reporter (1 μg/well), PRL-TK internal control (0.5 μg/well). After 48 h, the cells were treated with or without TNF-α for 15 min and the NF-κB transcriptional activity was analyzed using the Dual-Lumi Luciferase Reporter Gene Assay Kit. **E** The expression level of NS5A and its truncated mutants in above experiments was detected by Western blotting. Data presented as means ± SD. Statistical analyses were performed using GraphPad Prism version 6.01 software (GraphPad Software, La Jolla, CA, USA).**, $P < 0.01$; ***, $P < 0.001$; NS, not significant.

NEMO with NS5A. The ZF domain of NEMO is essential for the K63-polyubiquitination of NEMO and IKK activation induced by TNF-α (Tang et al., 2003; Cordier et al., 2009). Moreover, the K63-linked polyubiquitination of NEMO is needed for NF-κB activation (Ni et al., 2008). Therefore, we investigated whether NS5A inhibits NEMO K63-linked polyubiquitination. PK-15 cells and HEK293T cells were transfected with p3×FLAG-NS5A or p3×FLAG-cmv-10 vectors. At 36 h post-transfection, the cells were infected with SeV for 12 h (Fig. 10). Then, the cells were harvested for ubiquitination assay of NEMO. The results showed that the K63-linked polyubiquitination of NEMO remarkably decreased in the NS5A-expressing cells (Fig. 10).

4. Discussion

NF-κB plays a critical role in inflammation and the innate immune responses (Dev et al., 2011). Consequently, many viruses have developed various strategies targeting NF-κB to evade host immune response. The present study revealed that CSFV NS5A mediated the proteasomal degradation of NEMO and blocked the K63-linked polyubiquitination of NEMO, thereby inhibiting NF-κB signaling.

Dong and Tang (2016) reported that CSFV NS5A inhibited the degradation of IκBα, NF-κB nuclear translocation and transcriptional activity induced by poly(I:C) in PAM cells. The present study showed that NS5A blocked the IKK phosphorylation (Fig. 4A) and the degradation of IκBα (Fig. 4B) induced by TNF-α in HEK293T cells. These data indicated that NS5A may target an upstream event of IKK phosphorylation, such as IKK complex formation, NEMO ubiquitination, to inhibit the NF-κB signaling.

The N-terminal region of NEMO binds to the C-terminal segment (NEMO-binding domain, NBD) of IKKα and IKKβ to form the IKK complex and modulates IKK complex activity (Yamaoka et al., 1998). Previous studies demonstrate that the disruption of the association between NEMO and IKK inhibits the activation of IKK and NF-κB (May et al., 2000; Zhao et al., 2018; De Falco et al., 2016), thus we investigated whether the

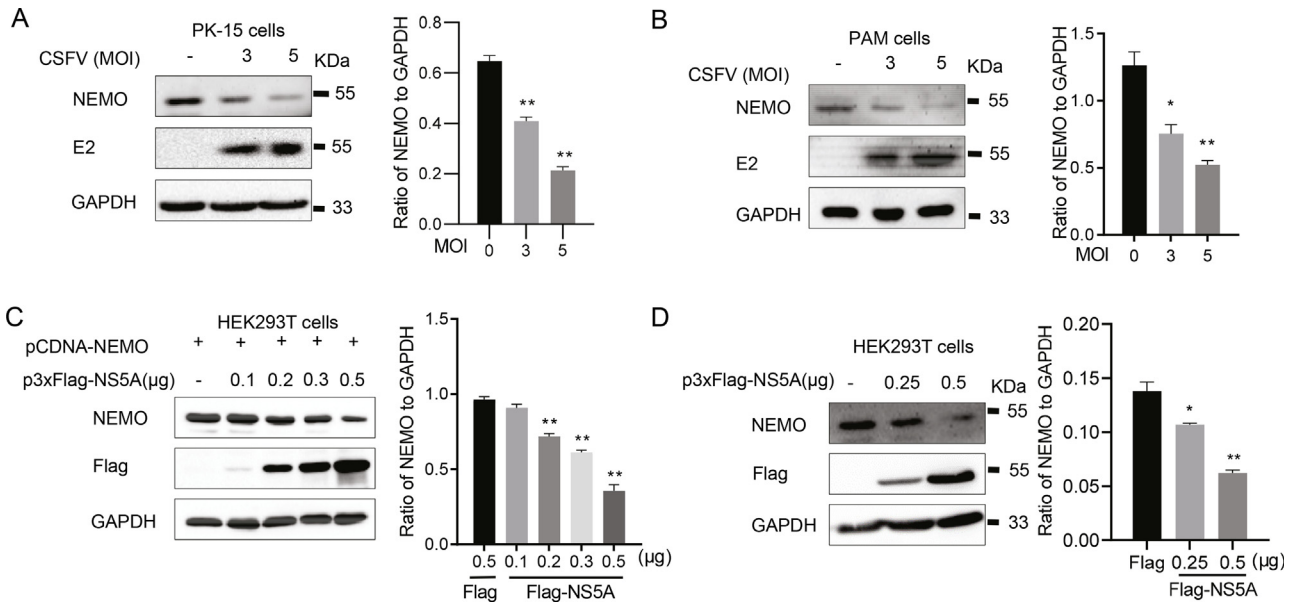

Fig. 5. Reduction of NEMO induced by CSFV or NS5A. PK-15 cells (**A**) or PAM cells (**B**) were infected with CSFV Shimen strain at an MOI of 3 or 5. At 48 hpi, the cells were lysed for Western blotting analysis with the indicated antibodies. **C, D** HEK293T cells cultured in 6-well plates were transfected with the indicated vector (pcDNA-NEMO, 2.5 μg/well). At 48 h post-transfection, the cells were lysed for Western blotting analysis with the indicated antibodies. Data presented as means ± SD. Statistical analyses were performed using GraphPad Prism version 6.01 software (GraphPad Software, La Jolla, CA, USA).*, $P < 0.05$; **, $P < 0.01$.

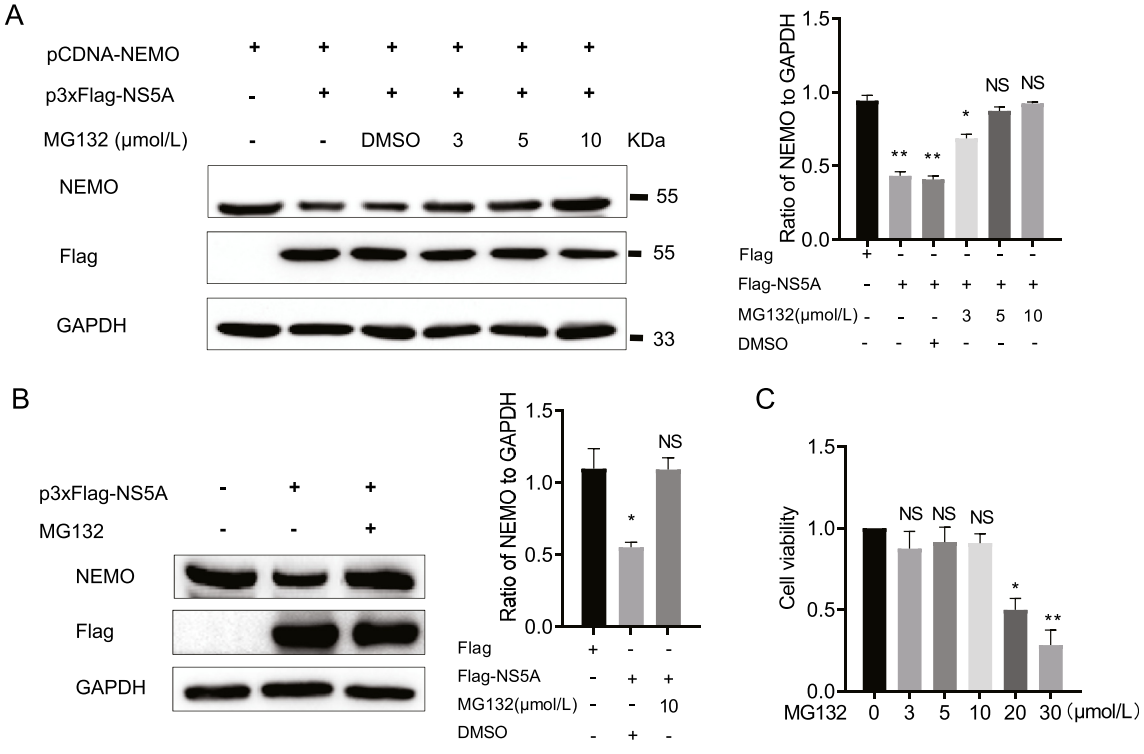

Fig. 6. NS5A mediates proteasomal degradation of NEMO. HEK293T cells cultured in 6-well plates were co-transfected with pcDNA-NEMO and p3×FLAG-NS5A vectors (2.5 μg/well) (**A**) or transfected with p3×FLAG-NS5A vector alone (2.5 μg/well) (**B**). At 24 h post-transfection, the cells were incubated with MG132 for 24 h, then the cells were lysed for Western blotting analysis with the indicated antibodies. **C** Cell viability after MG132 treatment was evaluated by MTT assay. Data presented as means ± SD. Statistical analyses were performed using GraphPad Prism version 6.01 software (GraphPad Software, La Jolla, CA, USA). *, $P < 0.05$; **, $P < 0.01$; NS, not significant.

interaction of CSFV NS5A with NEMO disrupts the association of NEMO with IKKα/IKKβ. Interaction assays indicated that the N-terminal region (aa 1–125) of NEMO containing the IKKα/IKKβ binding domain (aa 50–93) (May et al., 2000) is unnecessary for its interaction with NS5A (Fig. 2), which eliminates the likelihood that NS5A blocks the assembly of the IKK complex by binding to NEMO.

The critical role of NEMO in the activation of NF-κB signaling makes it an attractive target for viruses to inhibit NF-κB signaling. Some viruses, such as foot-and-mouth disease virus (Wang et al., 2012), porcine epidemic diarrhea virus (Wang et al., 2015) and porcine reproductive and respiratory syndrome virus (Huang et al., 2014) target NEMO and cleave it with their proteins with protease activity to inhibit the

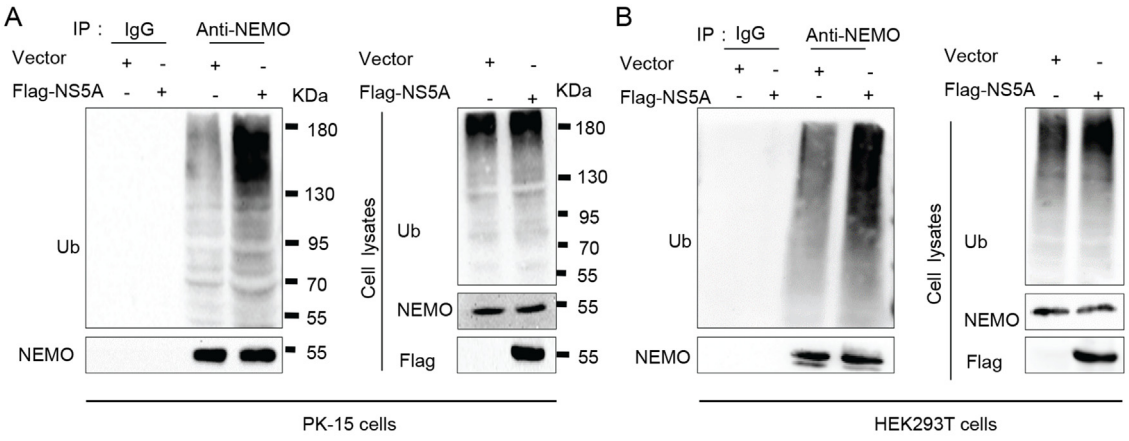

Fig. 7. NS5A mediates NEMO ubiquitination. PK-15 and HEK293T cells in 6-well plates were transfected with p3×FLAG-NS5A or p3×FLAG-CMV-10 (2.5 μg/well). At 24 h post-transfection, the cells were incubated with MG132 (10 μmol/L) for 24 h, and then the cells were lysed for immunoprecipitation with rabbit anti-NEMO mAb or nonspecific IgG. Western blotting analysis was performed by using mouse anti-Ub mAb, mouse anti-NEMO mAb and mouse anti-FLAG mAb.

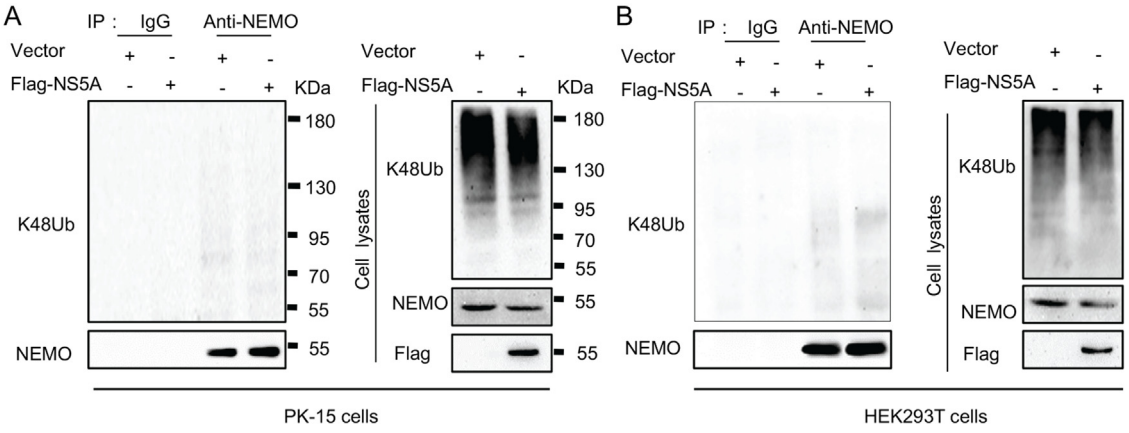

Fig. 8. NS5A does not mediate K48-linked polyubiquitination of NEMO. PK-15 and HEK293T cells in 6-well plates were transfected with p3×FLAG-NS5A or p3×FLAG-CMV-10 (2.5 μg/well). At 24 h post-transfection, the cells were incubated with MG132 (10 μmol/L) for 24 h. Then the cells were lysed for immunoprecipitation with rabbit anti-NEMO mAb, and Western blotting analysis was performed by using K48-linkage specific polyubiquitin (D9D5) rabbit mAb, mouse anti-NEMO mAb and mouse anti-FLAG mAb.

activation of IKK and NF-κB signaling. In addition, Brady et al. (2017) reported that molluscum contagiosum virus MC005 protein interacts with NEMO and blocks the conformational priming of the IKK kinase complex which occurs when NEMO couples to ubiquitin chains during NF-κB activation, thereby inhibiting IKK activation. The present study showed that CSFV or NS5A mediated the decrease in NEMO protein levels (Fig. 5) and the proteasome inhibitor MG132 could prevent this decrease (Fig. 6), indicating that NS5A mediates the proteasomal degradation of NEMO.

Ubiquitin, a highly conserved protein (76 aa), contains seven lysine residues and can form eight different types of polyubiquitin chains through the connection of the next ubiquitin molecule to one of its seven lysine residues (K6, K11, K27, K29, K33, K48, and K63) or N-terminus methionine (Met, linear). Different types of polyubiquitin chains mediate substrates toward distinct cellular pathways (Ohtake et al., 2018). Although some ubiquitin linkages are implicated in proteasomal degradation (Xu et al., 2009), K48 linkages act as the major signal for proteasomal degradation (Grice and Nathan, 2016). Accordingly, whether NS5A induces the K48-linked polyubiquitination of NEMO was first determined. Unexpectedly, NS5A does not mediate K48-linked polyubiquitination of NEMO (Fig. 8). Next, the type of polyubiquitination of NEMO mediated by NS5A was investigated and the results showed that NS5A induced the K27-linked polyubiquitination of NEMO for proteasomal degradation (Fig. 9). Similarly, Ashida et al. (2010) reported that IpaH9.8, a *Shigella* effector with E3 ligase activity, mediated the K27-linked polyubiquitination of NEMO by targeting K309 and K321 for proteasomal degradation, thus inhibiting NF-κB activation. Further study is needed to clarify whether NS5A mediates the K27-linked polyubiquitination of NEMO by targeting K309 and K321.

The ubiquitination of NEMO is essential for the activation of IKK induced by TNF-α (Tang et al., 2003; Hadian et al., 2011). Jun et al. (2013) showed that aside from the binding of NEMO to polyubiquitin chains coupled to RIP1, the site-specific ubiquitination of NEMO itself is essential for physiologic NF-kB signaling. Thus, viruses have evolved strategies to inhibit NF-κB signaling by blocking NEMO polyubiquitination. Biswas and Shisler (2017) reported that molluscum contagiosum virus MC159 protein binds to the N-terminal region of NEMO and blocks the interaction of NEMO with cIAP1, a cellular E3 ligase that mediates the K63-linked polyubiquitination of NEMO, resulting in the inhibition of IKK and NF-κB activation. Wu et al. (2021) showed that the SARS-CoV-2 ORF9b N-terminus interacts with NEMO and blocks its K63-linked polyubiquitination, leading to the inhibition of

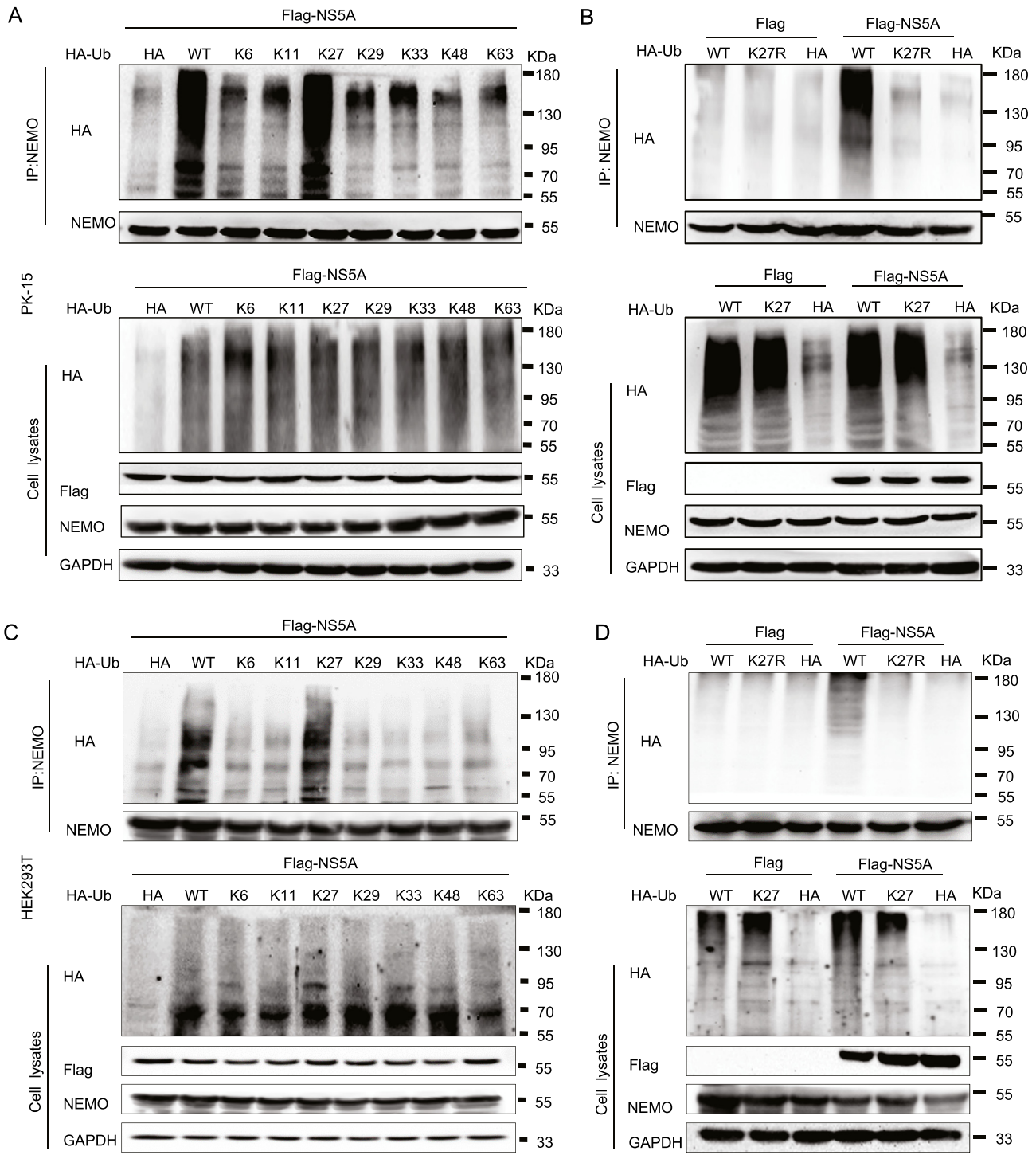

Fig. 9. NS5A induces K27-linked polyubiquitination of NEMO. PK-15 (**A** and **B**) and HEK293T (**C** and **D**) cells in 6-well plates were transfected with p3×FLAG-NS5A or p3×FLAG-CMV-10 (2.5 μg/well). At 24 h post-transfection, the cells were incubated with MG132 (10 μmol/L) for 24 h. Then the cells were harvested for immunoprecipitation with rabbit anti-NEMO mAb and ubiquitination assay of NEMO with mouse anti-HA mAb.

NF-κB signaling and IFN production. The present findings show that CSFV NS5A interacts with NEMO and the C-terminal ZF domain of NEMO is required for the interaction (Fig. 2B). Significantly, the ZF domain of NEMO is a functional ubiquitin-binding domain (Cordier et al., 2009) and an intact ZF of NEMO is essential for NEMO ubiquitination and the activation of IKK and NF-κB (Tang et al., 2003). As expected, the analysis of ubiquitination of NEMO showed that NS5A inhibited the K63-linked polyubiquitination of NEMO, resulting in the inhibition of NF-κB signaling (Fig. 10). These data highlight novel roles of NS5A in CSFV infection. It will be very meaningful to dissect how NS5A induces K27-linked polyubiquitination of NEMO and whether NS5A possesses ubiquitin ligase activity.

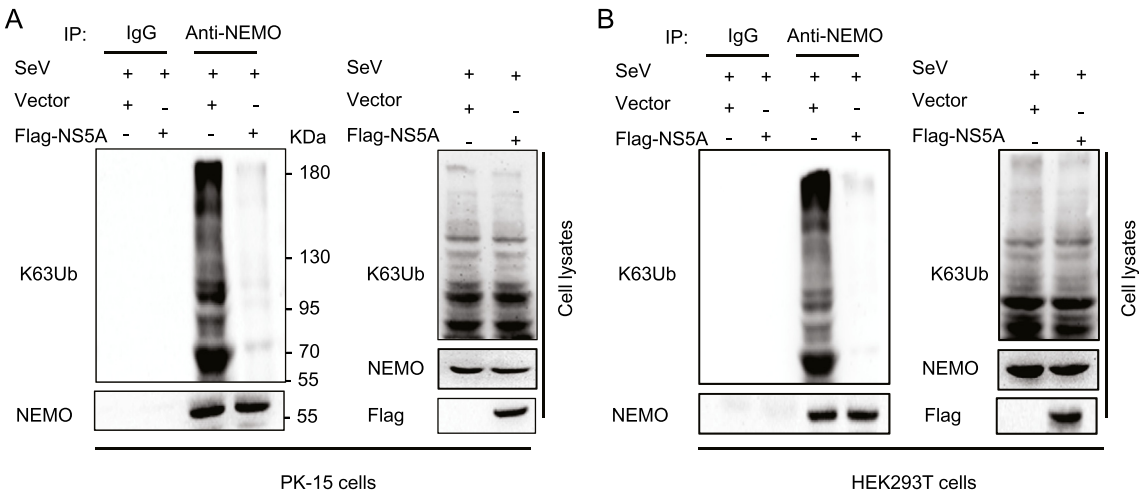

Fig. 10. NS5A inhibits K63-linked polyubiquitination of NEMO. PK-15 (**A**) and HEK293T (**B**) cells in 6-well plates were transfected with or without p3×FLAG-NS5A or p3×FLAG-CMV-10 vector (2.5 μg/well). Following incubation with MG132 (10 μmol/L) for 24 h and infection with SeV (500 HAU/well) for 12 h, the cells were lysed for immunoprecipitation with rabbit anti-NEMO mAb or nonspecific IgG, and Western blotting analysis was performed by using K63-linkage specific polyubiquitin (D7A11) rabbit mAb, and mouse anti-NEMO mAb or mouse anti-FLAG mAb.

5. Conclusions

In summary, this study has identified CSFV NS5A as a novel antagonist of innate immunity and has shown that NS5A inhibits the NF-κB signaling by mediating K27-linked polyubiquitination of NEMO for the proteasomal degradation and blocking the K63-linked polyubiquitination of NEMO. These findings reveal a novel mechanism by which CSFV evades the host innate immunity and contribute to better understanding of the pathogenesis of CSFV.

Data availability

All the data generated during the current study are included in the manuscript.

Ethics statement

This article does not contain any studies with human or animal subjects performed by any of the authors.

Author contributions

Jinfu Sun: conceptualization, methodology, writing-review & editing, supervision; Jiaying Li: investigation, methodology, validation; Liming Li: methodology, validation, writing-original draft; Haixiao Yu: investigation, formal analysis; Ping Ma: data curation, validation; Yingnan Wang: methodology, validation; Jinqi Zhu: investigation, methodology, validation; Zezhong Feng: validation, formal analysis; Changchun Tu: writing-review & editing, supervision.

Conflict of interest

The authors declare that they have no conflict of interest.

Acknowledgements

This work was supported by the National Nature Science Foundation of China (Grant No. 31972677) and the Construction Project of Liaoning Provincial Key Laboratory, China (2022JH13/10200026).

Appendix A. Supplementary data

Supplementary data to this article can be found online at https://doi.org/10.1016/j.virs.2023.09.002.

References

Alvarez, S.E., Harikumar, K.B., Hait, N.C., Allegood, J., Strub, G.M., Kim, E.Y., Maceyka, M., Jiang, H., Luo, C., Kordula, T., Milstien, S., Spiegel, S., 2010. Sphingosine-1-phosphate is a missing cofactor for the E3 ubiquitin ligase TRAF2. Nature 465, 1084–1088.

Ashida, H., Kim, M., Schmidt-Supprian, M., Ma, A., Ogawa, M., Sasakawa, C., 2010. A bacterial E3 ubiquitin ligase IpaH9.8 targets NEMO/IKKgamma to dampen the host NF-kappaB-mediated inflammatory response. Nat. Cell Biol. 12, 66–73.

Bertrand, M.J., Milutinovic, S., Dickson, K.M., Ho, W.C., Boudreault, A., Durkin, J., Gillard, J.W., Jaquith, J.B., Morris, S.J., Barker, P.A., 2008. cIAP1 and cIAP2 facilitate cancer cell survival by functioning as E3 ligases that promote RIP1 ubiquitination. Mol. Cell 30, 689–700.

Biswas, S., Shisler, J.L., 2017. Molluscum contagiosum virus MC159 abrogates cIAP1-NEMO interactions and inhibits NEMO polyubiquitination. J. Virol. 91 e002766-17.

Brady, G., Haas, D.A., Farrell, P.J., Pichlmair, A., Bowie, A.G., 2017. Molluscum contagiosum virus protein MC005 inhibits NF-κB activation by targeting NEMO-regulated IκB kinase activation. J. Virol. 91 e005455-17.

Chen, L.J., Dong, X.Y., Zhao, M.Q., Shen, H.Y., Wang, J.Y., Pei, J.J., Liu, W.J., Luo, Y.W., Ju, C.M., Chen, J.D., 2012a. Classical swine fever virus failed to activate nuclear factor –kappa b signaling pathway both in vitro and in vivo. Virol. J. 9, 293.

Chen, Y., Xiao, J., Xiao, J., Sheng, C., Wang, J., Jia, L., Zhi, Y., Li, G., Chen, J., Xiao, M., 2012b. Classical swine fever virus NS5A regulates viral RNA replication through binding to NS5B and 3'-UTR. Virology 432, 376–388.

Chiaravalli, J., Fontan, E., Fsihi, H., Coic, Y.M., Baleux, F., Véron, M., Agou, F., 2011. Direct inhibition of NF-κB activation by peptide targeting the NOA ubiquitin binding domain of NEMO. Biochem. Pharmacol. 82, 1163–1174.

Ciechanover, A., 2005. Proteolysis: from the lysosome to ubiquitin and the proteasome. Nat. Rev. Mol. Cell Biol. 6, 79–87.

Cordier, F., Grubisha, O., Traincard, F., Véron, M., Delepierre, M., Agou, F., 2009. The zinc finger of NEMO is a functional ubiquitin-binding domain. J. Biol. Chem. 284, 2902–2907.

De Falco, F., Di Giovanni, C., Cerchia, C., De Stefano, D., Capuozzo, A., Irace, C., Iuvone, T., Santamaria, R., Carnuccio, R., Lavecchia, A., 2016. Novel non-peptide small molecules preventing IKKβ/NEMO association inhibit NF-κB activation in LPS-stimulated J774 macrophages. Biochem. Pharmacol. 104, 83–94.

Dev, A., Iyer, S., Razani, B., Cheng, G., 2011. NF-κB and innate immunity. Curr. Top. Microbiol. Immunol. 349, 115–143.

Dong, X.Y., Tang, S.Q., 2016. Classical swine fever NS5A protein changed inflammatory cytokine secretion in porcine alveolar macrophages by inhibiting the NF-kB signaling pathway. Virol. J. 13, 101.

Dong, X.Y., Liu, W.J., Zhao, M.Q., Wang, J.Y., Pei, J.J., Luo, Y.W., Ju, C.M., Chen, J.D., 2013. Classical swine fever virus triggers RIG-I and MDA5-dependent signaling pathway to IRF-3 and NF-κB activation to promote secretion of interferon and inflammatory cytokines in porcine alveolar macrophages. Virol. J. 10, 286.

Ea, C.K., Deng, L., Xia, Z.P., Pineda, G., Chen, Z.J., 2006. Activation of IKK by TNFalpha requires site-specific ubiquitination of RIP1 and polyubiquitin binding by NEMO. Mol. Cell 22, 245–257.
Fan, Y., Yu, Y., Shi, Y., Sun, W., Xie, M., Ge, N., Mao, R., Chang, A., Xu, G., Schneider, M.D., Zhang, H., Fu, S., Qin, J., Yang, J., 2010. Lysine 63-linked polyubiquitination of TAK1 at lysine 158 is required for tumor necrosis factor alpha- and interleukin-1beta-induced IKK/NF-kappaB and JNK/AP-1 activation. J. Biol. Chem. 285, 5347–5360.
Grassmann, C.W., Isken, O., Tautz, N., Behrens, S.E., 2001. Genetic analysis of the pestivirus nonstructural coding region: defects in the NS5A unit can be complemented in trans. J. Virol. 75, 7791–7802.
Grice, G.L., Nathan, J.A., 2016. The recognition of ubiquitinated proteins by the proteasome. Cell. Mol. Life Sci. 18, 3497–3506.
Hadian, K., Griesbach, R.A., Dornauer, S., Wanger, T.M., Nagel, D., Metlitzky, M., Beisker, W., Schmidt-Supprian, M., Krappmann, D., 2011. NF-κB essential modulator (NEMO) interaction with linear and lys-63 ubiquitin chains contributes to NF-κB activation. J. Biol. Chem. 286, 26107–26117.
Huang, C., Zhang, Q., Guo, X.K., Yu, Z.B., Xu, A.T., Tang, J., Feng, W.H., 2014. Porcine reproductive and respiratory syndrome virus nonstructural protein 4 antagonizes beta interferon expression by targeting the NF-κB essential modulator. J. Virol. 88, 10934–10945.
Iwasaki, A., Medzhitov, R., 2010. Regulation of adaptive immunity by the innate immune system. Science 327, 291–295.
Jun, J.C., Kertesy, S., Jones, M.B., Marinis, J.M., Cobb, B.A., Tigno-Aranjuez, J.T., Abbott, D.W., 2013. Innate immune-directed NF-κB signaling requires site-specific NEMO ubiquitination. Cell Rep. 4, 352–361.
Le Negrate, G., 2012. Viral interference with innate immunity by preventing NF-kB activity. Cell Microbiol. 14, 168–181.
Li, S., Wang, J., He, W.R., Feng, S., Li, Y., Wang, X., Liao, Y., Qin, H.Y., Li, L.F., Dong, H., Sun, Y., Luo, Y., Qiu, H.J., 2015. Thioredoxin 2 is a novel E2-interacting protein that inhibits the replication of classical swine fever virus. J. Virol. 89, 8510–8524.
Liu, X., Wang, X., Wang, Q., Luo, M., Guo, H., Gong, W., Tu, C., Sun, J., 2018. The eukaryotic translation initiation factor 3 subunit E binds to classical swine fever virus NS5A and facilitates viral replication. Virology 515, 11–20.
May, M.J., D'Acquisto, F., Madge, L.A., Glöckner, J., Pober, J.S., Ghosh, S., 2000. Selective inhibition of NF-kappaB activation by a peptide that blocks the interaction of NEMO with the IkappaB kinase complex. Science 289, 1550–1554.
Muñoz-González, S., Ruggli, N., Rosell, R., Pérez, L.J., Frías-Leuporeau, M.T., Fraile, L., Montoya, M., Cordoba, L., Domingo, M., Ehrensperger, F., Summerfield, A., Ganges, L., 2015. Postnatal persistent infection with classical swine fever virus and its immunological implications. PLoS One 10, e0125692.
Napetschnig, J., Wu, H., 2013. Molecular basis of NF-κB signaling. Annu. Rev. Biophys. 42, 443–468.
Ni, C.Y., Wu, Z.H., Florence, W.C., Parekh, V.V., Arrate, M.P., Pierce, S., Schweitzer, B., Van Kaer, L., Joyce, S., Miyamoto, S., Ballard, D.W., Oltz, E.M., 2008. Cutting edge: K63-linked polyubiquitination of NEMO modulates TLR signaling and inflammation in vivo. J. Immunol. 180, 7107–7111.
Ohtake, F., Tsuchiya, H., Saeki, Y., Tanaka, K., 2018. K63 ubiquitylation triggers proteasomal degradation by seeding branched ubiquitin chains. Proc. Natl. Acad. Sci. USA 115, 1401–1408.
Sapay, N., Montserret, R., Chipot, C., Brass, V., Moradpour, D., Deléage, G., Penin, F., 2006. NMR structure and molecular dynamics of the in-plane membrane anchor of nonstructural protein 5A from bovine viral diarrhea virus. Biochemistry 45, 2221–2233.
Sheng, C., Zhu, Z., Yu, J., Wan, L., Wang, Y., Chen, J., Gu, F., Xiao, M., 2010. Characterization of NS3, NS5A and NS5B of classical swine fever virus through mutation and complementation analysis. Vet. Microbiol. 140, 72–80.
Sheng, C., Chen, Y., Xiao, J., Wang, J., Li, G., Chen, J., Xiao, M., 2012. Classical swine fever virus NS5A protein interacts with 3'-untranslated region and regulates viral RNA synthesis. Virus Res. 163, 636–643.
Sheng, C., Kou, S., Jiang, Q., Zhou, C., Xiao, J., Li, J., Chen, B., Zhao, Y., Wang, Y., Xiao, M., 2014. Characterization of the C-terminal sequence of NS5A necessary for the assembly and production of classical swine fever virus infectious particles. Res. Vet. Sci. 97, 449–454.
Sheng, C., Liu, X., Jiang, Q., Xu, B., Zhou, C., Wang, Y., Chen, J., Xiao, M., 2015. Annexin A2 is involved in the production of classical swine fever virus infectious particles. J. Gen. Virol. 96, 1027–1032.
Takaesu, G., Surabhi, R.M., Park, K.J., Ninomiya-Tsuji, J., Matsumoto, K., Gaynor, R.B., 2003. TAK1 is critical for IkappaB kinase-mediated activation of the NF-kappaB pathway. J. Mol. Biol. 326, 105–115.
Tang, E.D., Wang, C.Y., Xiong, Y., Guan, K.L., 2003. A role for NF-kappaB essential modifier/IkappaB kinase-gamma (NEMO/IKKgamma) ubiquitination in the activation of the IkappaB kinase complex by tumor necrosis factor-alpha. J. Biol. Chem. 278, 37297–37305.
Tautz, N., Tews, B.A., Meyers, G., 2015. The molecular biology of pestiviruses. Adv. Virus Res. 93, 47–160.
Tellinghuisen, T.L., Paulson, M.S., Rice, C.M., 2006. The NS5A protein of bovine viral diarrhea virus contains an essential zinc-binding site similar to that of the hepatitis C virus NS5A protein. J. Virol. 80, 7450–7458.
Wajant, H., Scheurich, P., 2011. TNFR1-induced activation of the classical NF-κB pathway. FEBS J. 278, 862–876.
Wang, X., Robbins, J., 2014. Proteasomical and lysosomical protein degradation and heart disease. J. Mol. Cell. Cardiol. 71, 16–24.
Wang, C., Deng, L., Hong, M., Akkaraju, G.R., Inoue, J., Chen, Z.J., 2001. TAK1 is a ubiquitin-dependent kinase of MKK and IKK. Nature 412, 346–351.
Wang, D., Fang, L., Li, K., Zhong, H., Fan, J., Ouyang, C., Zhang, H., Duan, E., Luo, R., Zhang, Z., Liu, X., Chen, H., Xiao, S., 2012. Foot-and-mouth disease virus 3C protease cleaves NEMO to impair innate immune signaling. J. Virol. 86, 9311–9322.
Wang, D., Fang, L., Shi, Y., Zhang, H., Gao, L., Peng, G., Chen, H., Li, K., Xiao, S., 2015. Porcine epidemic diarrhea virus 3C-like protease regulates its interferon antagonism by cleaving NEMO. J. Virol. 90, 2090–2101.
Wu, J., Shi, Y., Pan, X., Wu, S., Hou, R., Zhang, Y., Zhong, T., Tang, H., Du, W., Wang, L., Wo, J., Mu, J., Qiu, Y., Yang, K., Zhang, L.K., Ye, B.C., Qi, N., 2021. SARS-CoV-2 ORF9b inhibits RIG-I-MAVS antiviral signaling by interrupting K63-linked ubiquitination of NEMO. Cell Rep. 34, 108761.
Xu, P., Duong, D.M., Seyfried, N.T., Cheng, D., Xie, Y., Robert, J., Rush, J., Hochstrasser, M., Finley, D., Peng, J., 2009. Quantitative proteomics reveals the function of unconventional ubiquitin chains in proteasomal degradation. Cell 137, 133–145.
Yamaoka, S., Courtois, G., Bessia, C., Whiteside, S.T., Weil, R., Agou, F., Kirk, H.E., Kay, R.J., Israël, A., 1998. Complementation cloning of NEMO, a component of the IκB kinase complex essential for NF-κB activation. Cell 93, 1231–1240.
Zhang, L., Zhao, D., Jin, M., Song, M., Liu, S., Guo, K., Zhang, Y., 2020. Rab18 binds to classical swine fever virus NS5A and mediates viral replication and assembly in swine umbilical vein endothelial cells. Virulence 11, 489–501.
Zhao, J., Zhang, L., Mu, X., Doebelin, C., Nguyen, W., Wallace, C., Reay, D.P., McGowan, S.J., Corvo, L., Clemens, P.R., Wilson, G.M., Watkins, S.C., Solt, L.A., Cameron, M.D., Huard, J., Niedernhofer, L.J., Kamenecka, T.M., Robbins, P.D., 2018. Development of novel NEMO-binding domain mimetics for inhibiting IKK/NF-κB activation. PLoS Biol. 16, e2004663.
Zhuo, Y., Guo, Z., Ba, T., Zhang, C., He, L., Zeng, C., Dai, H., 2021. African swine fever virus MGF360-12L inhibits type I interferon production by blocking the interaction of importin α and NF-κB signaling pathway. Virol. Sin. 36, 176–186.